Flow sources of wall pressure fluctuations resolved by DDES in a reattaching flow region

T. T. Tran, R. Perrin, R. Manceau, J. Borée, P. Jordan

International Symposium
On Turbulence and Shear Flow
Phenomena (TSFP-8)
August 28 - 30, 2013 Poitiers, France

FLOW SOURCES OF WALL PRESSURE FLUCTUATIONS RESOLVED BY DDES IN A REATTACHING FLOW REGION

T. Tran[1] T, R. Perrin[1], R. Manceau[1,2], J. Borée[1], P. Jordan[1]

[1] Institut Pprime, UPR CNRS 3346, CNRS, ISAE - ENSMA, Université de Poitiers,
BP 40109, 86961 Futuroscope Chasseneuil Cedex, France

[2] Lab. de mathématiques et de leur applications (LMA)
CNRS-Université de Pau et des pays de l'Adour
IPRA, avenue de l'université 60013 Pau, France

rodolphe.perrin@univ-poitiers.fr

ABSTRACT

This paper is concerned with the analysis of the flow structures responsible for the wall pressure fluctuations predicted by DDES near a reattachment. To this aim, a simulation of the flow over a thick plate is considered. It observed that the linear part of sources is dominant upstream of the reattachment, and that quadratic sources dominate downstream. This is associated with the rapid loss of coherence of the vortices shed from the separated shear layer in the downstream region. Furthermore, it is shown that linear stochastic estimation of the velocity field from the wall pressure well reproduce the linear sources, with negligible quadratic sources.

INTRODUCTION

The work reported in this paper is concerned, on a general level, with the problem posed by our increasing ability to compute and/or measure turbulent flows with high space- and time-resolution: perspicacious analysis and data-reduction methodologies are paramount. From the full complexity of the turbulence, measured or computed, it is necessary to distill the essential mechanisms with regard to the problem at hand, or an observable of particular interest. It is by means of such distillation that reduced complexity models can be proposed, eventually with a view to addressing the problem of control. We consider flow over a blunt flat plate (fig. 1) at high Reynolds number, which we compute using DDES, and our goal is to probe the flow with regard to the flow structures that underpin the wall pressure fluctuations; the latter phenomenon is treated as an observable that we use to educe, from the broad range of turbulent motions, only those by which it is driven.

This two-dimensional separation-reattachment flow has been the subject of much research in the past (Kiya and Sasaki 1983, Cherry, Hiller and Latour 1984, Hudy, Naguib and Humphreys 2007), and the question regarding the turbulence flow sources of hydrodynamic wall pressure fluctuations continues to be a subject of academic interest. The mean reattachment is responsible for a rapid longitudinal evolution of the spatiotemporal organisation of these sources; the flow thus presents a considerable challenge in terms of both its computation and its analysis.

Possibly one of the most widely-used feature-eduction techniques found in the literature is conditional analysis, perfectly suited for the task described above: an observable is chosen and used to conditionally sample some related field. Linear stochastic estimation is an interesting tool in this regard: it allows the computation of an approximation of a conditional field using an observable that can be spatiotemporally distributed. Two recent examples can be found in Sicot, Perrin, Tran & Borée (2012) and Kerhervé et al (2012). In the former paper an experimental data base, acquired in the same research project that supported the present work (ANR DIB), was processed using an adapted multi-time, multi-point stochastic estimation of the velocity field associated with the fluctuating wall pressure; the conditional field obtained comprised large-scale vortices shed from the separated shear layer.

In this paper we consider the sources of hydrodynamic wall pressure fluctuations predicted by DDES. Using the velocity field computed by the DDES we compute both the linear and quadratic contributions to the wall pressure fluctuations; we do so using a technique taken from the aeroacoustics literature (Lee & Ribner 1972), where the contributions are computed by means of pressure-velocity correlations: the observable is thus used to compute its source. The nature of the sources, and in particular the relative contributions of the linear and quadratic components, are shown to evolve strongly from upstream to downstream of the reattachment point. The same pressure-velocity correlations are then used to compute a conditional velocity field, by means of linear stochastic estimation, with respect to the pressure fluctuations at the reattachment point; the pressure source terms associated with the conditional field are computed and compared with those of the complete flow. The linear source terms of the full and conditional velocity fields are identical (this can be demonstrated formally), suggesting that the conditional field computed by stochastic estimation may provide access to the space-time flow motions associated with the linear pressure term of the complete flow (these motions are not directly accessible from the raw data ; i.e. while it is straightforward to compute the linear source terms from a given flow realisation, it is not straightforward to educe the space-time field that contributes to the source term.) The conditional field does not, on the other hand, comprise a quadratic source term.

FLOW CONFIGURATION AND NUMERICAL ASPECTS

The flow configuration is presented in figure 1. The Reynolds number, based on the upstream velocity U_∞ and the plate thickness e, is $Re = U_\infty e/\nu = 80,000$. The extent of the computational domain is $Lx = 70e$, $Ly = 31e$ and $Lz = 3.5e$, with an inlet located $30e$ upstream of the stagnation point. Preliminary 2D URANS tests have shown that such an extent is necessary to ensure that the results are independent of the size of the domain. The boundary conditions are inflow/outflow in the x-direction and free-slip in the y-direction. Since the reference experiment was performed using a relatively large aspect ratio ($\simeq 30$), homogeneity in the z-direction in the central part of the plate is assumed, such that periodicity is imposed in the z-direction.

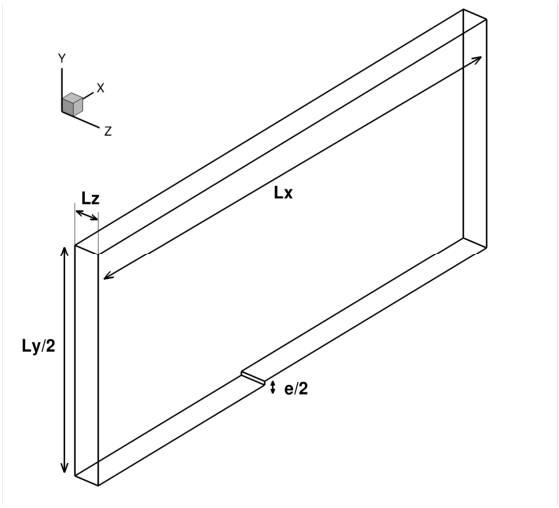

Figure 1 : Flow configuration

The simulations have been performed using *Code_Saturne*, developed at EDF (Archambeau & al, 2004), an unstructured, collocated finite-volume code, which is second order accurate in time and space, and uses a SIMPLEC type algorithm, with a Rhie and Chow procedure. The flow has been investigated using URANS and DDES approaches both based on the SST model (Menter, 1994). The DDES model that has been implemented uses the shield function proposed by Spalart & al (2006), rather than the function F_2 of the SST model, mainly because the protected RANS region has been found less extended using the Spalart function, hence accelerating the transition from a RANS to a LES behavior. For the convection scheme, the blending proposed by Travin & al (2000) which switches from a TVD scheme in the RANS region to a centered scheme in LES regions has been used. The grid contains approximately 2.5 million cells, refined near the wall to achieve a y^+ value of order 1. The time step was set to $10^{-3}e/U_\infty$ and independence of the statistical quantities with regards to the time step have been checked. After a transient period of approximately $100e/U_\infty$, statistical averaging has been performed over a period of 400 e/U_∞, which represents approximately 50 shedding periods downstream of the mean reattachment. The convergence of the statistics is also enhanced by averaging along the z direction.

The simulation is found in good agreement with the experimental study (Sicot & al, 2012) carried out during the same project (ANR DIB). The mean reattachment length is found at $x \approx 5.7\ e$, in good agreement with the experiment ($\approx$5.5e) and with the literature. Figure 2 shows longitudinal mean velocity profiles at different x positions. As expected, the agreement is found much better than that achieved with a RANS model, even if the boundary layer recovery seems to be slightly anticipated with DDES.

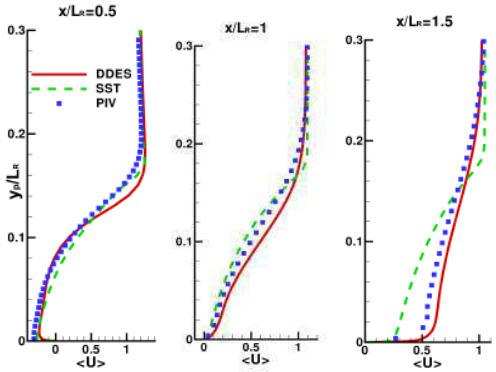

Figure 2 : Mean longitudinal velocity profiles.

Spectra of velocity components in the outer layer at the mean reattachment have been plotted in Figure 3, and a good agreement is again achieved with experiment, even if the broadband contribution corresponding to vortex shedding downstream of the reattachment, is found in a slightly higher Strouhal number range ($St=f\ e/U_\infty \approx 0.15$-0.2) that in the experiment of Sicot & al, 2012 ($St=f\ e/U_\infty \approx 0.1$-0.15). A more detailed analysis of the simulation compared to experiment can be found in Tran (2012), where it was concluded that the large scales of the fluctuating motion is well predicted by DDES.

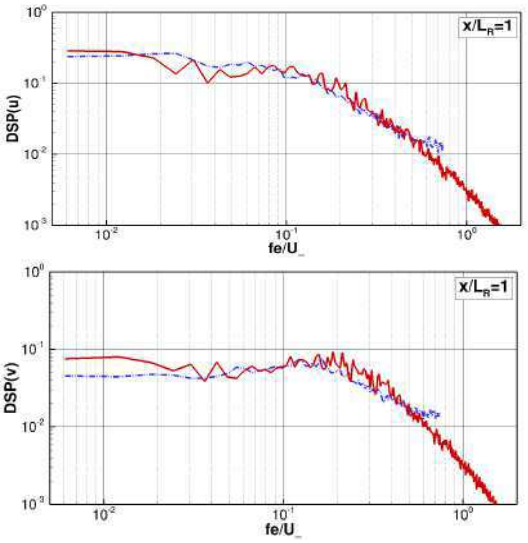

Figure 3 : Spectra of velocity in the shear layer above the mean reattachment.
Blue line: experiment, red line: simulation.
(top: u component, bottom: v component)

Figure 4 shows the longitudinal evolution of the fluctuating wall pressure coefficient *Cp'*. In agreement with the literature, the maximum is found just upstream of the mean reattachment, and a strong decrease is observed downstream. This has been attributed to a rapid loss of coherence, after the reattachment, of the shed structures emanating from the shear layer (Sicot & al, 2012). The maximum value of *Cp'* is slightly overestimated by the simulation. A possible explanation will be given in the following section.

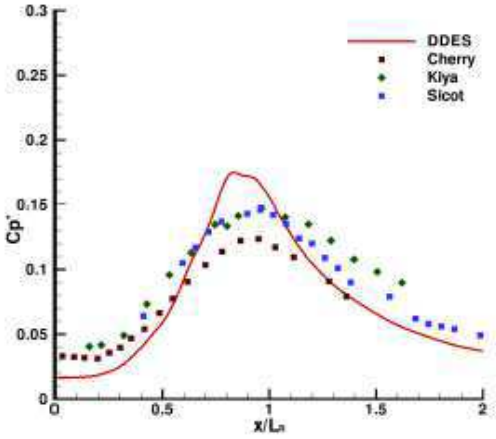

Figure 4 : Predicted Cp' versus experimental data

DETERMINATION AND ANALYSIS OF THE SOURCES OF WALL FLUCTUATING PRESSURE

The wall region analysed here surrounds the mean reattachment point located at $x = L_R = 5.5e$. Neglecting the contribution of the leading edge and of the Stokes terms at the wall (Naguib and Koochesfahani 2004), the wall fluctuating pressure at a location **x** reads :

$$p(\mathbf{x},t) = -\frac{\rho}{2\pi}\int_V \frac{q(\mathbf{x}',t)}{\|\mathbf{x}'-\mathbf{x}\|}d\mathbf{x}'$$

where

$$q = -2\rho u_{i,j}\langle U_{j,i}\rangle + \rho\left(-u_{i,j}u_{j,i} + \langle u_{i,j}u_{j,i}\rangle\right)$$

$$= q_L + q_Q \qquad (1)$$

q_L and q_Q are respectively the linear and quadratic contributions to *p*. Strictly speaking, using DDES velocity fields, this equation should be completed by terms coming from the modeled turbulent stresses. For a first approach, we have chosen to neglect these terms, which seems to be justified by the fact that the integration of the source terms described in the following restitutes correct values of C_p'. The focus of this paper is thus the flow sources of wall pressure fluctuations resolved by the present DDES approach in a reattaching flow region. We insist on the fact that such methodology is valid to test any hybrid RANS-LES or LES results in such a challenging situation.

Following eq. (1), the variance $\langle p^2(\mathbf{x})\rangle$ reads:

$$\langle p^2(\mathbf{x})\rangle = \frac{\rho^2}{4\pi^2}\int_V\int_V \frac{\langle q(\mathbf{x}',t)q(\mathbf{x}'',t)\rangle}{\|\mathbf{x}'-\mathbf{x}\|\|\mathbf{x}''-\mathbf{x}\|}d\mathbf{x}'d\mathbf{x}''$$

$$= \frac{\rho^2}{4\pi^2}\int_V\int_V S_{\mathbf{x}}(\mathbf{x}',\mathbf{x}'')d\mathbf{x}'d\mathbf{x}'' \qquad (2)$$

In relation (2),

$$\langle qq\rangle = \langle q_Lq_L\rangle + \langle q_Lq_Q\rangle + \langle q_Qq_L\rangle + \langle q_Qq_Q\rangle.$$

The four contributions to $S_{\mathbf{x}}(\mathbf{x}',\mathbf{x}'')$, correspond to all combinations of linear and quadratic cross-correlation terms. These two-point correlations are thoroughly studied in Tran (2012). We present here, as examples, the contributions to $\langle p^2(\mathbf{x})\rangle$ at the reattachment (x=Lr) as functions of $\Delta x'' = x'' - x$ and $\Delta z'' = z'' - z$ with respectively $\mathbf{x}' = (L_R, 0.02L_R, 0)$ - *fig. 5a and 6a* - *and* $\mathbf{x}' = (L_R, 0.1L_R, 0)$ *fig. 5b and 6b.* $y = 0.02L_R$ approximately corresponds to the average boundary of the "LES region" of the DDES computation while $y = 0.1L_R$ approximately corresponds to the location of the maximum mean shear $\partial\langle U\rangle/\partial y$ at mean reattachment. We clearly see that the cross correlations between linear and quadratic terms are weak when compared to linear-linear and quadratic-quadratic correlations. They will therefore be neglected in what follows. Moreover, we see that the two-point contributions rapidly decay in space when the separation between **x''** and **x'** increases. "Integral length scales" can be computed from the corresponding correlation coefficients and are found to be of order *0.02*L_R.

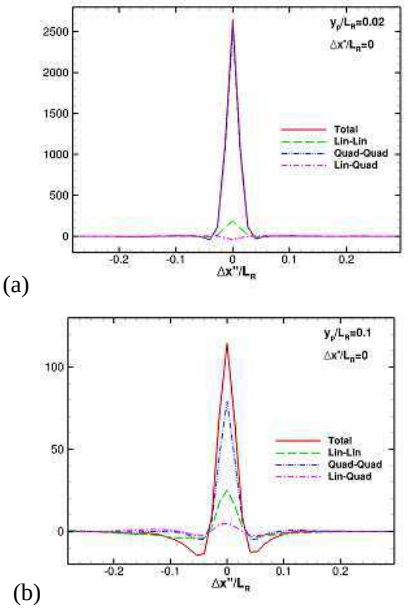

Figure 5 : Longitudinal profiles of the contributions to $\langle p^2(\mathbf{x})\rangle$ at the reattachment with $\mathbf{x}' = (L_R, 0.02L_R, 0)$ - fig. 5a - and $\mathbf{x}' = (L_R, 0.1L_R, 0)$ - fig. 5b - respectively.

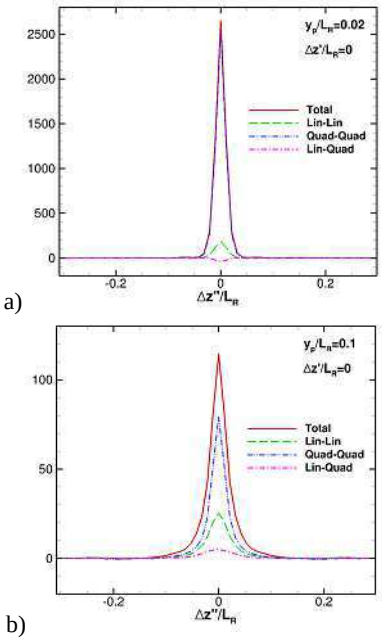

Fig. 6 : Spanwise profiles of the contributions to $\left\langle p^2(\mathbf{x})\right\rangle$ at the reattachment with $\mathbf{x}'=(L_R,0.02L_R,0)$ - fig. 6a - and $\mathbf{x}'=(L_R,0.1L_R,0)$ - fig. 6b - respectively.

Equation (2) can therefore be written in a simpler form as :

$$\left\langle p^2(\mathbf{x})\right\rangle = -\frac{\rho}{2\pi}\int_V \frac{\left\langle q(\mathbf{x}',t)p(\mathbf{x},t)\right\rangle}{\left\|\mathbf{x}'-\mathbf{x}\right\|}d\mathbf{x}'$$
$$. = \int_V D_{\mathbf{x}}(\mathbf{x}')d\mathbf{x}'$$
$$= \int_V \left[D_{\mathbf{x}}{}^{L}(\mathbf{x}')+D_{\mathbf{x}}{}^{Q}(\mathbf{x}')\right]d\mathbf{x}' \qquad (3)$$

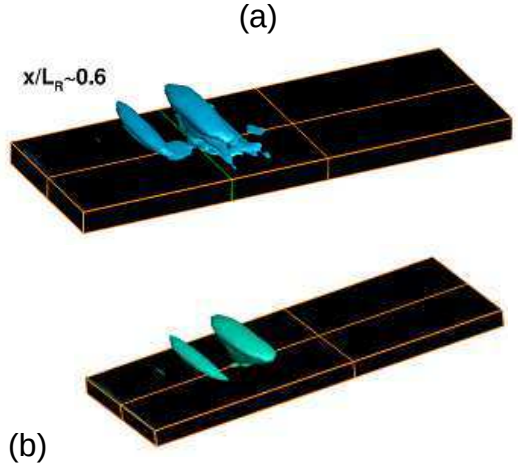

Fig. 7 : Iso-surface of $\hat{D}_{\mathbf{x}}(\mathbf{x}')=D_{\mathbf{x}}(\mathbf{x}')\Big/\left\langle p^2(\mathbf{x})\right\rangle = 2/\pi$ at $x=0.6L_R$. (a), total contribution; (b) linear contribution.

We insist on the fact that, despite the non-local nature of pressure in the correlation $\left\langle q(\mathbf{x}',t)p(\mathbf{x},t)\right\rangle$, $D_{\mathbf{x}}(\mathbf{x}')$ can be considered as a local contribution because two-point <*qq*> correlations decay very rapidly in space. Moreover, it can be split rigorously into linear $D_{\mathbf{x}}{}^{L}$ and quadratic $D_{\mathbf{x}}{}^{Q}$ contribution because correlations between linear and quadratic terms are found negligible. An iso-surface of $\hat{D}_{\mathbf{x}}(\mathbf{x}')=D_{\mathbf{x}}(\mathbf{x}')\Big/\left\langle p^2(\mathbf{x})\right\rangle$ at $x=0.6L_R$ is shown in fig. 7. At this point on the wall well under the recirculating region, we observe the signature of outer events having a significant spanwise extent. The distributions of $\hat{D}_{\mathbf{x}}(\mathbf{x}')$, $\hat{D}_{\mathbf{x}}{}^{L}(\mathbf{x}')$ and $\hat{D}_{\mathbf{x}}{}^{Q}(\mathbf{x}')$ in longitudinal and spanwise vertical planes for $x=0.6L_R$ are shown in fig. 8. The linear contribution has a very organized signature in the shear layer (fig. 7b and 8b). $D_{\mathbf{x}}{}^{L}(\mathbf{x}')\propto -\left\langle q^L(\mathbf{x}',t)p(0.6L_R,t)\right\rangle$ is indeed positive above $x=0.6L_R$ because organized Kelvin-Helmholtz vortices produce significant contributions to $\left\langle p^2\right\rangle$. In this linear contribution, negative regions of $-\left\langle q^L(\mathbf{x}',t)p(0.6L_R,t)\right\rangle$ correspond to straining regions between two large scale structures. Noting that $-\left\langle pq_L\right\rangle = 2\rho\left\langle \mathbf{u_i}p\right\rangle_{,\mathbf{j}}\left\langle \mathbf{U_j}\right\rangle_{,\mathbf{i}}$ and that the dominant mean velocity gradient is the mean shear $\partial\langle U\rangle/\partial y$, such observations are expected and explain the lateral coherence observed in fig. 7a and b.

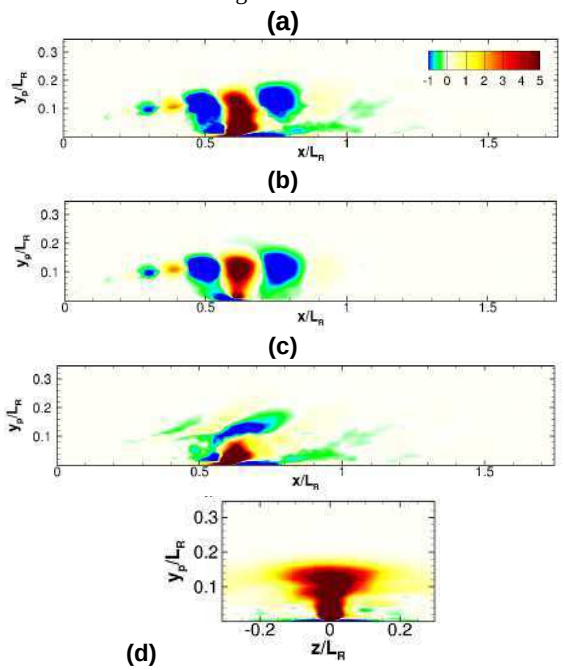

Figure 8 : Distributions of $D_{\mathbf{x}}(\mathbf{x}')$ (a), $D_{\mathbf{x}}{}^{L}(\mathbf{x}')$ (b) and $D_{\mathbf{x}}{}^{Q}(\mathbf{x}')$ (c) in a longitudinal vertical plane for $x=0.6L_R$. (8d) distribution of $D_{\mathbf{x}}(\mathbf{x}')$ in the spanwise vertical plane for $x=L_R$.

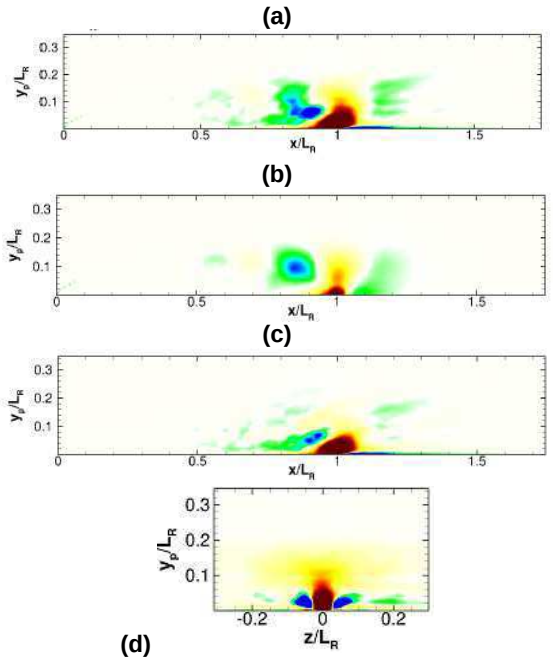

Figure 9: Distributions of $D_{\mathbf{x}}(\mathbf{x}')$ (a), $D_{\mathbf{x}}{}^{L}(\mathbf{x}')$ (b) and $D_{\mathbf{x}}{}^{Q}(\mathbf{x}')$ (c) in a longitudinal vertical plane for $x=L_R$. (9d) distribution of $D_{\mathbf{x}}(\mathbf{x}')$ in the spanwise vertical plane for $x=L_R$.

Distributions of $\hat{D}_{\mathbf{x}}(\mathbf{x}')$ in longitudinal and spanwise vertical planes at the location of the mean reattachment point ($x=L_R$) are shown in fig. 9. The linear contribution is much weaker and the non-linear terms dominate nearer to the wall. With the present DDES results, a conditional structure based on an event of second quadrant ($u.v<u_{rms}v_{rms}$) at $x=L_R$ and $y=0.1\ L_R$ (maximum mean shear) was obtained (Adrian 1979). Figure 10 shows that this conditional structure has the shape of an hairpin. This observation is consistent with the experimental findings of (Kiya and Sasaki 1985). A refined analysis shows that the spanwise distance between the "legs" of this conditional structure is $0.08L_R$. In fig. 9d, the spanwise distance between the dominant positive contribution to $\hat{D}_{\mathbf{x}}(\mathbf{x}')$ and the localized lateral negative contributions is $0.04L_R$. Such a distance could therefore correspond to the average spanwise location of significant straining regions when a vortex tube is located above the considered wall location and contributes significantly to $\langle p^2 \rangle$. This shows that the correct prediction of flow sources of wall pressure fluctuations in the reattachment region (and downstream it) critically depends on the ability of the DDES model to predict such longitudinal near wall structuration. In particular, many authors (e.g. Shur & al, 2008, Piomelli & al, 2003) have shown that in channel flow simulations, a DES model predicts unphysical very elongated streaks. Even if the situation is different in this case (reattachment), it is likely that the non-linear terms are strongly affected by these artificial structures. This can also explain the overestimation of *Cp'* observed in fig. 4. Therefore, the sources educed here have to be interpreted as sources predicted by a DDES model and an extrapolation to physical mechanisms would require further tests, using models that does not predict such structures, for instance IDDES (Shur & al 2008) or PITM (Fadai-Gotbi & al, 2010).

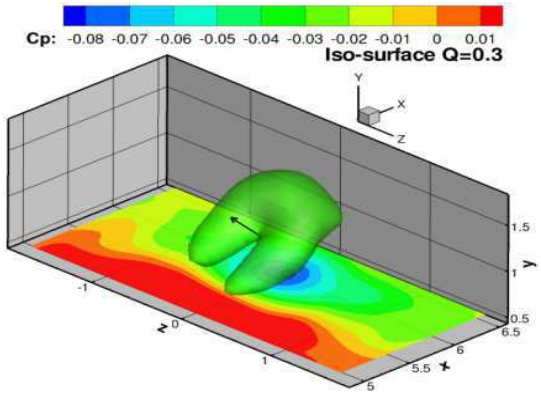

Fig. 10 : Conditional Q and wall fluctuating pressure iso-contours. The condition for an event of second quadrant is $u.v<-u_{rms}v_{rms}$ at $x/L_R=1$ and $y/L_R=0.1$ (maximum shear).

At each location at the wall $\mathbf{x}=(x,0,0)$ and for $x\in[0.6L_R,1.4L_R]$, the linear and quadratic contributions to $\langle p^2(x)\rangle$ can be integrated (the integration domain being restricted to $x\pm L_R/2$). Fig. 11 shows the relative contribution of linear and quadratic terms to $\langle C_p{}^2 \rangle$. One sees that the dominant contribution switches from linear to quadratic downstream of the mean reattachment point and that $\langle C_p{}^2 \rangle$ decreases very fast in this region.

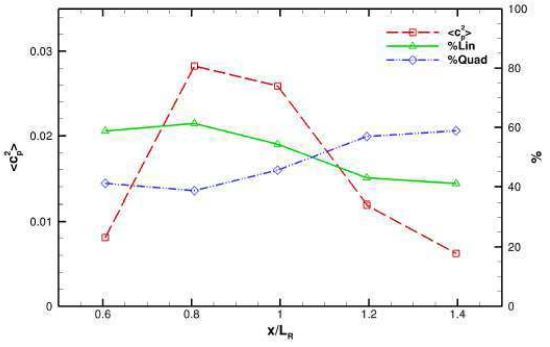

Fig. 11 : Longitudinal evolution of $\langle C_p{}^2 \rangle$ (left axis) and relative contributions of linear and quadratic terms (%, right axis) to $\langle C_p{}^2 \rangle$

Linear stochastic estimation tools are often used in order to reconstruct conditional velocity fields from wall pressure array measurements (Hudy et al. 2007, Sicot et al. 2012) and to analyze the relationship between the shed structures and the fluctuating wall pressure. Any linear stochastic estimation (or related linear statistical methodologies) $\tilde{\mathbf{u}}_\mathbf{i}$ of the velocity field $\mathbf{u}_\mathbf{i}$ from the wall fluctuating pressure field then satisfies the property: $\langle \mathbf{u_i} p \rangle = \langle \tilde{\mathbf{u}}_\mathbf{i} p \rangle$. Therefore, it is easy to show that:

$$-\langle pq_L \rangle = 2\rho \langle \mathbf{u}_\mathbf{i} p \rangle_{,\mathbf{j}} \langle \mathbf{U}_\mathbf{j} \rangle_{,\mathbf{i}}$$

$$= 2\rho \langle \tilde{\mathbf{u}}_\mathbf{i} p \rangle_{,\mathbf{j}} \langle \mathbf{U}_\mathbf{j} \rangle_{,\mathbf{i}} = -\langle p\tilde{q}_L \rangle \qquad (4)$$

This shows that the linear contribution of estimated fields is equal to the exact linear contribution. This statement has been confirmed by computing flow sources from a multi-time and multi-channel stochastic estimation of the DDES velocity field correlated with the wall pressure in Tran, 2012. Corresponding graphs are not shown here for brevity. Moreover, as any linearly estimated velocity field appears to be filtered at large scales, we have observed that the quadratic contribution of $\tilde{\mathbf{u}}_\mathbf{i}$ is negligible. The rapid loss of coherence of estimated flow structures downstream the reattachment region (Sicot et al. 2012) is therefore associated to the strong decay of linear flow sources after reattachment.

CONCLUSION

Flow sources responsible for the wall pressure fluctuations were evaluated on the basis of a DDES simulation. It has been shown that the linear sources dominate upstream of the mean reattachment, while the quadratic terms dominate downstream, due to the rapid loss of coherence of the shed vortices in this region.

This paper is restricted to the analysis of the flow predicted by a DDES model. Further studies should consider simulations using different hybrid approaches, especially in order to evaluate the influence of the model on the quadratic part. More generally, the same methodology can also be applied to LES or DNS at lower Reynolds number.

ACKNOWLEDGMENT

This study was conducted during the french ANR contract DIB (Dynamic Unsteadiness Noise) under the contract ANR-07-BLAN-0177.

This work was granted access to the HPC resources of IDRIS under the allocation 2010-020912 made by GENCI (Grand Equipement National de Calcul Intensif).

REFERENCES

Adrian, R. J., 1979, “Conditional eddies in isotropic turbulence", Phys. of Fluids **22**: 2065-2070.

Archambeau, F., Méchitoua, N. & Sakiz M., 2004, Code Saturne: A Finite Volume Code for the Computation of Turbulent Incompressible Flows – Industrial Applications. Int. J. on Finite Volume, Electronical Edition: http://averoes.math.univ-paris13.fr/html **ISSN 1634** (0655)

Cherry, N. J., Hillier R. and Latour M., 1984, "Unsteady measurements in a separated and reattaching flow", J. Fluid Mech. **144**: 13-46.

Fadai-Ghotbi A., Friess C., Manceau R., Borée J., 2010, "A seamless hybrid RANS-LES model based on transport equations for the subgrid stresses and elliptic blending." Physics of Fluids, vol. 22(no. 5).

Hudy, L. M., Naguib A. N. and Humphreys W. M., 2007, "Stochastic estimation of a separated-flow field using wall-pressure-array measurements", Phys. of Fluids **19-2**.

Kerhervé F., Jordan P., Cavalieri A. V. G., Delville J., Bogey C., Juvé D. (2012) "Educing the source mechanism associated with downstream radiation in subsonic jets", JFM 170:606-640.

Kiya, M. and Sasaki K., 1983, "Structure of a turbulent separation bubble", J. Fluid Mech. **137**: 83-113.

Kiya, M. and Sasaki K., 1985, "Structure of large scale vortices and unsteady reverse flow in the reattaching zone of a turbulent separation bubble.", J. Fluid Mech. **154**: 463-491.

Lee H K and Ribner H S, 1972, "Direct correlation of noise and flow of a jet", J. Acoust. Soc. Am. 52:1280-90.

Menter, F. R., 1994, "Two-equation eddy-viscosity turbulence models for engineering aplications", AIAA J. **32 (8)**: 1598-1605.

Naguib, A. N. and Koochesfahani M. M., 2004, "On wall-pressure sources associated with the unsteady separation in a vortex-ring/wall interaction", Phys. of Fluids **16-7**: 2613-2622.

Piomelli U., Balaras E., Pasinato H., Squires K., Spalart P. R., 2003, "The inner outer layer interface in large-eddy simulations with wall-layer models"; Int. J. Heat and Fluid Flow, vol. 24 :pp. 538-550.

Shur M. L., Spalart P. R., Strelets M. K., Travin A. K., 2008, "A hybrid RANS LES approach with delayed-DES and wall-modelled LES capabilities", Int. Journal of Heat and Fluid Flow, vol. 29 p. 1638-1649.

Sicot, C., Perrin R., Tran T. T. and Borée J., 2012, "Wall pressure and conditional flow structures in the reattachment region of the flow over a thick plate", Int. Journal of Heat and Fluid Flow, vol. 35, p. 119 - 129.

Spalart, P. R., Deck S., Shur M., Squires K. D., Strelets M. and Travin A. , 2006, "A new version of detached-eddy simulation, resistant to ambiguous grid densities", Theor. and Comp. Fluids Dyn. **20**: 181-195.

Tran, T. T., 2012, "Modélisation Hybride RANS/LES d'écoulements massivement décollés en régime turbulent. Etude des corrélations pression/vitesse et confrontation à l'expérimentation", PhD Thesis - ISAE-ENSMA.

Travin, A., Shur, M., Strelets, M., Spalart, P. R., 2000. "Physical and numerical upgrades in the detached-eddy simulation of complex turbulent flows". Proc. 412th Euromech Coll. LES an Complex Transitional and Turbulent Flows, Munich, Germany.